

Instruments and Methods

Towards radiocarbon dating of ice cores

M. SIGL,^{1,2,3} T.M. JENK,⁴ T. KELLERHALS,^{1,2} S. SZIDAT,¹ H.W. GÄGGELER,^{1,2}
L. WACKER,⁵ H.-A. SYNAL,⁵ C. BOUTRON,⁶ C. BARBANTE,^{7,8} J. GABRIELI,⁷
M. SCHWIKOWSKI^{2,3}

¹Department of Chemistry and Biochemistry, University of Bern, CH-3012 Bern, Switzerland

²Paul Scherrer Institut, CH-5232 Villigen PSI, Switzerland

E-mail: margit.schwikowski@psi.ch

³Oeschger Centre for Climate Change Research, University of Bern, CH-3012 Bern, Switzerland

⁴Centre for Ice and Climate, Niels Bohr Institute, University of Copenhagen, DK-2100 Copenhagen, Denmark

⁵Ion Beam Physics, ETH Hönggerberg, CH-8093 Zürich, Switzerland

⁶Laboratoire de Glaciologie et Géophysique de l'Environnement du CRNS (associé à l'Université Joseph Fourier – Grenoble I),
54 Rue Molière, BP 96, 38402 Saint-Martin-d'Hères Cedex, France

⁷Environmental Sciences Department, University of Venice, I-30123 Venice, Italy

⁸Institute for the Dynamics of Environmental Processes – CNR, University Ca' Foscari of Venice, 30123 Venice, Italy

ABSTRACT. A recently developed dating method for glacier ice, based on the analysis of radiocarbon in carbonaceous aerosol particles, is thoroughly investigated. We discuss the potential of this method to achieve a reliable dating using examples from a mid- and a low-latitude ice core. Two series of samples from Colle Gnifetti (4450 m a.s.l., Swiss Alps) and Nevado Illimani (6300 m a.s.l., Bolivian Andes) demonstrate that the ¹⁴C ages deduced from the water-insoluble organic carbon fraction represent the age of the ice. Sample sizes ranged between 7 and 100 µg carbon. For validation we compare our results with those from independent dating. This new method is thought to have major implications for dating non-polar ice cores in the future, as it provides complementary age information for time periods not accessible with common dating techniques.

1. INTRODUCTION

Glaciers and ice sheets around the world contain information about a broad variety of environmental conditions during the Earth's past. Analyses of polar ice cores not only provide insights into forcing factors affecting past climate (e.g. greenhouse gases, volcanic and solar activity), but also allow temperature reconstructions going back several hundred thousand years (EPICA Community Members, 2004; Brook, 2005; Bard and Frank, 2006; Muscheler and others, 2007; Masson-Delmotte and others, 2009). High-alpine ice cores from mid- and low-latitude glaciers and ice caps provide complementary information, as they are able to capture regional climate signals (e.g. aerosol forcing) in areas inhabited by the majority of the world's population (Thompson and others, 2006a).

Appropriate and precise depth–age models are essential for any such palaeo-environmental studies. In polar ice cores this can be achieved using a combination of annual-layer counting on seasonally varying parameters (e.g. $\delta^{18}\text{O}$), matching signals to well-established chronologies and ice-flow modelling (Meese and others, 1997; Vinther and others, 2006; Parrenin and others, 2007). Those techniques are, however, often inapplicable for high-alpine ice cores where glacier flow is dominated by the small-scale geometry of bedrock, resulting in a strongly non-linear depth–age relationship. These difficulties cannot be resolved fully using ice-flow models (Lüthi and Funk, 2001). In addition, the formation of clear annual signals within the archive is often hampered by the strongly varying distribution of snowfall as well as by post-depositional changes (e.g. wind erosion) that

frequently occur in high-alpine environments (Wagenbach and Geis, 1989; Maupetit and others, 1995; Döschner and others, 1996). Reference horizons (e.g. bomb peaks, volcanic eruptions) give additional dating constraints, but their identification is not always straightforward given the higher background level of most chemical compounds in the atmosphere of the mid-latitudes. To our knowledge, volcanic eruptions have not yet been identified in non-polar ice cores prior to AD 1258. Radiometric methods such as ²¹⁰Pb offer an alternative independent option as they are not affected by such limitations, but they are restricted temporally to about only 200 years back (Gäggeler and others, 1983; Eichler and others, 2000). For longer timescales, radiocarbon dating has been applied successfully to several ice cores, where sufficient carbon-containing material was incorporated. Suitable material included wood fragments or insects (Thompson and others, 1998, 2002, 2006b), although it is emphasized that macrofossils in ice cores appear rather rarely.

Carbonaceous particles are a major component of naturally occurring aerosols that are emitted ubiquitously or formed in the atmosphere, and that reach potential ice-core sites (Seinfeld and Pandis, 1998; Lavanchy and others, 1999; Jenk and others, 2006; Legrand and others, 2007; McConnell and others, 2007). According to their thermal and optical properties, the particles are classified as organic carbon (OC, hydrocarbons of low to medium molecular weight) or elemental carbon (EC, highly polymerized hydrocarbons). OC and EC have different sources. In pre-industrial times, OC was emitted predominantly from the terrestrial biosphere as primary aerosol or formed in the

atmosphere as secondary aerosol from gaseous precursors, whereas the main source of EC was pyrolysis during combustion. Residence times of aerosols in the atmosphere are in the order of several days. Therefore, altering of the ^{14}C signature of the aerosols between emission and their deposition is unlikely. This reduces potential reservoir effects to a minimum. Concentrations of water-insoluble OC and EC have been analysed in various snow-pit samples and ice cores. In Greenland, concentrations of OC vary about $4\text{ }\mu\text{g kg}^{-1}$ (Hagler and others, 2007) while for the Alps concentrations of up to $60\text{ }\mu\text{g kg}^{-1}$ were determined (Jenk and others, 2006). Differences were explained by the distances of the archive from major source regions. Concentrations of EC are generally lower, and range between 0.2 and $2.0\text{ }\mu\text{g kg}^{-1}$ in Greenland (Chýlek and others, 1995; Hagler and others, 2007) and $\sim 30\text{ }\mu\text{g kg}^{-1}$ in the Alps (Jenk and others, 2006). In the recent past a strong temporal variability of carbon concentrations is observed in ice cores, related to anthropogenic emissions (Lavanchy and others, 1999; Jenk and others, 2006; McConnell and others, 2007). By determining the $^{14}\text{C}/^{12}\text{C}$ ratios of subsequent samples of OC for the period AD 1650–1900 from a well-dated ice core from the Swiss Alps (Fiescherhorn, 3900 m a.s.l.), it was shown that the OC incorporated in ice is almost of purely biogenic origin before about AD 1850 (Jenk and others, 2006), making this fraction a valuable target for age determination. The applied method, based on accelerator mass spectrometry (AMS) ^{14}C dating on samples at a microgram carbon level after previous thermal separation of OC from EC, is described in detail elsewhere and has been thoroughly validated (Jenk and others, 2007).

In this study we discuss the application of the ^{14}C dating technique to an ice core from Nevado Illimani (Andes, 6300 m a.s.l.) and the previously dated ice core from Colle Gnifetti (Alps, 4450 m a.s.l.) (Jenk and others, 2009). For validation purposes we analysed various individual samples from Greenland (GRIP, Greenland Ice Core Project) with good independent age control (Vinther and others, 2006). Low OC concentrations and potential sample contamination during processing are the major challenges of the method. The latter can be quantified, and a blank estimation for correction is presented here. Finally, $^{14}\text{C}/^{12}\text{C}$ ratios from the separated EC fractions are compared with those of OC, to evaluate the potential to use total carbon ($\text{TC} = \text{OC} + \text{EC}$) for dating as proposed by Steier and others (2006). The aim of this paper is to give a critical evaluation of the potential of this new dating method. Developing final depth–age models for both ice cores requires the integration of various sources of site-specific chronological information, which is done elsewhere (Kellerhals, 2008; Jenk and others, 2009).

2. STUDY SITES AND SAMPLE SELECTION

Sample sequences from two ice cores are analysed in this study. The first study site is Nevado Illimani (16.62°S , 67.77°W), a permanently covered ice cap in the Bolivian Andes, where two parallel ice cores (to depths of 136.7 and 138.7 m) were drilled in 1999 in a joint expedition of the Paul Scherrer Institut (PSI, Switzerland) and the Institut de Recherche pour le Développement (IRD, France). Description of site characteristics, first dating models and climatic interpretations exist for both cores (De Angelis and others,

2003; Knüsel and others, 2003; Ramirez and others, 2003; Knüsel and others, 2005). The Amazon basin upwind of the ice-core site is considered to be a main source of carbonaceous aerosols (Graham and others, 2003; Guyon and others, 2004). Starting at bedrock, a continuous sequence of nine samples from the 138.7 m (113.2 m w.e.) long core was analysed for ^{14}C . Additionally, three samples also include a well-known dating horizon (volcanic eruption, AD 1258) for cross-validation. Length and masses of the ice sections range from 0.2 to 0.7 m and 0.3 to 1.2 kg, respectively. The variations are due to varying ice quality, limited sample amounts and unknown a priori information about the actual carbon concentrations.

The second study site is Colle Gnifetti, a cold glacier saddle in the Swiss/Italian Alps (45.93°N , 7.88°E), intensively studied and characterized during past decades (Oeschger and others, 1977; Alean and others, 1983; Haeberli and Alean, 1985; Wagenbach and Geis, 1989; Wagner, 1994; Döschner and others, 1996; Schwikowski and others, 1999; Lüthi and Funk, 2001; Eisen and others, 2003; Barbante and others, 2004). It was shown that the study site preferentially accumulates summer snow, whereas winter snow is likely to be eroded by strong winds. During summer, the impurities scavenged from precipitation mainly derive from terrestrial sources around southern central Europe (Lugauer and others, 1998). These aerosol sources could also be tracked by chemical transport models (ECHAM5) (Fagerli and others, 2007). Long-range transport is dominated by episodic airborne dust events, the source of which is the Saharan region (Wagenbach and Geis, 1989; Sodemann and others, 2006). Carbonaceous aerosols are expected to have similar source regions and pathways. From an 82 m (62.8 m w.e.) long ice core drilled in 2003 on a location where the oldest ice was expected, a nearly continuous sequence of the deepest 15 m was analysed for this study. Sizes of the 13 samples range between 0.5 and 1.1 kg. Nine of these samples were used for a first dating application of the method discussed here (Jenk and others, 2009).

For method validation, ice sections from Greenland (GRIP, 3230 m a.s.l.; 72.58°N , 37.64°W) were analysed. Eight time windows covering most of the Holocene were selected and two consecutive sections each of about 0.5 m ice were processed as one sample of approximately 2 kg mass. A larger sample amount was chosen, as OC concentrations are expected to be low at Summit in Greenland (Hagler and others, 2007).

We also discuss two ^{14}C samples from another Andean ice core (Mercedario, 6100 m a.s.l.; 31.97°S , 70.12°W , drilled in 2005) with an estimated age of 100 ± 10 years using conventional annual-layer counting. Sample details together with the results are listed in Tables 1–3.

3. METHODS

3.1. Carbonaceous particle extraction and OC/EC separation

The method used in this study relies on techniques that were primarily developed to attribute sources of ambient aerosols from air filters by tracking their carbon contents isotopically (Szidat and others, 2004a,b). A two-step combustion performed with the THEODORE system (Szidat and others, 2004c) allows a separation of OC from EC. By measuring the $^{14}\text{C}/^{12}\text{C}$ ratios of the two particulate carbon fractions, the

contribution of fossil vs biogenic sources can be estimated, assuming a contemporary $^{14}\text{C}/^{12}\text{C}$ ratio for biogenic and a ^{14}C extinct signal for anthropogenic (fossil) carbon (Reddy and others, 2002; Szidat and others, 2006). First applications on snow and ice samples were realized by Biegalski and others (1998) and Slater and others (2002). For the adaptation to ice-core samples the original method was modified. A detailed description of the method and a complete overview of essential corrections are presented by Jenk and others (2007). All steps described below were carried out under clean-room conditions (<100 particles per ft^3 (i.e. per $2.83 \times 10^{-2} \text{ m}^3$) with size $>0.5 \mu\text{m}$; US FED STD 209E class 100) in a laminar flow box using material of quartz, glass, stainless steel or Teflon. Filtration material was cleaned prior to use by rinsing several times with ultra-pure water (18 M Ω cm quality) and preheating. In brief, ice-core sections were decontaminated by removing the outer parts with a bandsaw before rinsing the samples with ultra-pure water. After filtration of the liquid samples using freshly preheated quartz fibre filters (Pallflex Tissuquartz, 2500QAO-UP), carbonates were removed by acidifying three times with 50 μL of 0.2 M HCl. During a stepwise combustion in an oxygen stream (10 min at 340°C; 12 min at 650°C) OC is separated from EC and the resulting CO_2 of each fraction is trapped cryogenically and quantified manometrically. The detection limit is $\sim 0.2 \mu\text{g}$. The CO_2 samples are sealed in glass ampoules for final ^{14}C determination by accelerator mass spectrometry (AMS) at the ETH Laboratory of Ion Beam Physics.

3.2. ^{14}C analysis

Analyses were performed between December 2005 and September 2008. Some of the early samples were measured on a 500 kV pelletron compact system 'TANDY' (Synal and others, 2000) after reduction of the CO_2 sample to a solid graphite target. Although there are suitable catalysts available for reducing small to ultra-small CO_2 samples (Santos and others, 2007a), reduction of CO_2 from ice samples often showed low efficiencies. In particular, samples with a high dust load were characterized by low yields of carbon due to interfering sulfur species during graphitization (Jenk and others, 2007). As significant fractionation occurred as a consequence of incomplete graphitization, additional corrections had to be applied using $\delta^{13}\text{C}$ measured by isotope ratio mass spectrometry on sample aliquots. On an individual ice-core sample from Colle Gnifetti, sources and magnitudes of errors leading to the final dating uncertainty were stepwise estimated and quantified (Jenk and others, 2007; Wacker and others, in press). To overcome such limitations, since December 2006 samples have been analysed using the 200 kV compact radiocarbon system 'MICADAS' with a gas ion source (Ruff and others, 2007; Synal and others, 2007), allowing direct measurement of gaseous samples of 3–30 μg with an uncertainty level as low as 1%. Where sample sizes were above 30 μg , which is the limit of the syringe used in the gas-handling system, the CO_2 was split into several glass ampoules and measured consecutively. Performance tests of the AMS system were run with various reference materials in which reproducible values, in agreement with the consensus values, could be achieved for solid and gaseous targets (Jenk and others, 2007; Ruff and others, 2007). The novel AMS system has an approximately four times lower blank than typical blanks of solid targets (Ruff and others, in

press). Additionally, the gas blanks seem to be independent of the sample sizes in the range 5–30 μg . This means that the current-dependent blank and standard corrections of AMS measurements applied in the past for small graphite targets (Jenk and others, 2007) are no longer necessary, thus further reducing the final dating uncertainty (Ruff and others, 2007, in press).

While recent developments in AMS techniques allow measurements down to below 2 μg with a precision as high as 1% for 10 μg samples (Santos and others, 2007a,b), the most important limitation remains the overall procedural blank (involving all steps starting with the cutting of the ice until the final AMS analysis), which is often one to two orders of magnitude higher than the machine background (Currie, 2000). Contamination with either modern or fossil carbon, in principle possible at each step of sample processing, will influence the final results, especially considering the low carbon concentrations expected in ice-core samples (Slater and others, 2002; Steier and others, 2006). Therefore, a low and reproducible procedural blank is required to minimize uncertainties of the obtained radiocarbon ages (Jenk and others, 2007). A procedural blank was estimated using artificial ice blocks of frozen ultra-pure water which have been treated the same way as real ice samples. However, reliable ^{14}C measurements require a minimum sample amount of at least 3 μg at the actual performance level of our AMS system (Ruff and others, 2007). Accordingly, filters from two to four blank ice filtrations were pooled for a single AMS measurement. Before any series of ice samples was processed, one procedural blank was determined to assure the quality of the THEODORE system. Including the previously reported values (Jenk and others, 2007), the procedural blank was re-evaluated in this study and is now based on a total of 20 measurements of the mass of carbon contamination and nine determinations of its isotopic composition. The correction we finally applied to the AMS results due to the procedural blank is:

$$f_{\text{M corrected}} = \frac{m_{\text{C}} \cdot f_{\text{M initial}} - m_{\text{procedural blk}} \cdot f_{\text{M procedural blk}}}{m_{\text{C}} - m_{\text{procedural blk}}},$$

where f_{M} denotes the $^{14}\text{C}/^{12}\text{C}$ ratio observed relative to the ratio of the reference year 1950 and m_{C} denotes the carbon mass separated for AMS analysis. Modern carbon is defined as $f_{\text{M}}=1$, while fossil carbon is noted with $f_{\text{M}}=0$. For detailed information on the definition of f_{M} see Donahue and others (1990).

All conventional ^{14}C ages were calibrated using OxCal 4.1 software (Bronk Ramsey, 2001) with the IntCal04 calibration curve (Reimer and others, 2004). As the Southern Hemispheric calibration curve is temporally restricted to the last 11 000 years (McCormac and others, 2004), samples from the Andean ice core were calibrated using the IntCal04 calibration curve. Considering the location of the drilling site with its carbon sources near the Equator and the small age deviation between the two calibration curves at 10 000 BP of about 30 years, this is not regarded as important with respect to the final dating uncertainties of the ice samples.

All radiocarbon-derived dates are presented as calibrated ages (cal BP = 1950) with a 1σ range as defined by Stuiver and Polach (1977), if not quoted otherwise. When comparing radiocarbon-derived ages with historical events (e.g. volcanic eruptions) we use calendar ages (AD).

Table 1. Summary of the Colle Gnifetti 2003 ice-core samples, which were analysed by ^{14}C dating including the samples previously analysed and discussed (Jenk and others, 2009). Absolute uncertainties indicate the 1σ range

Core section	Depth m w.e.	Ice kg	Carbon fraction	Carbon $\mu\text{g kg}^{-1*}$ μg		AMS label	Radiocarbon f_M	^{14}C age years BP	Calibrated age [†] years BP = 1950
102–104	49.4–51.1	1.111	OC	22.6	26.6	EG0753	0.872 ± 0.018	1100 ± 160	800–1240
			EC	14.6	16.5	EG0746	0.876 ± 0.018	1060 ± 160	800–1170
105/106	51.1–52.2	1.055	OC	16.5	17.1	EG0221	0.947 ± 0.043	435 ± 365	<690
			EC	8.4	10.4		Sample lost during processing		
107	52.3–52.8	0.500	OC	13.8	7.3	EG0099	$0.974 \pm 0.051^{\S}$	$210 \pm 420^{\S}$	<510
109	53.4–54.1	0.588	OC	15.5	9.5	EG0098	0.922 ± 0.038	650 ± 330	320–930
107+109	52.3–54.1	1.088	EC	9.5	10.4	EG0100	0.771 ± 0.017	2090 ± 170	1890–2310
110/111	54.1–55.3	0.929	OC	23.4	23.2	EG0754	0.874 ± 0.019	1080 ± 180	800–1220
			EC	14.8	14.1	EG0747	0.877 ± 0.019	1060 ± 170	800–1170
112/113	55.3–56.5	1.003	OC	30.7	32.2		Sample lost during processing		
			EC	22.1	22.5	EG0748	0.824 ± 0.015	1560 ± 140	1310–1600
114	56.5–57.0	0.902	OC	31.3	28.6	ET691[‡]	0.859 ± 0.036	1220 ± 330	790–1480
			EC	16.7	16.3	ET690 [‡]	0.780 ± 0.037	2000 ± 380	1520–2450
115/116	57.0–58.1	0.953	OC	43.6	43.1	EG0755	0.656 ± 0.013	3390 ± 160	3460–3840
			EC	23.1	22.3	EG0749	0.844 ± 0.015	1370 ± 140	1090–1410
117	58.1–58.4	0.904	OC	36.2	33.1	ET553[‡]	0.805 ± 0.029	1740 ± 290	1350–1990
			EC	25.4	24.2	ET557 [‡]	0.706 ± 0.026	2800 ± 300	2520–3360
121	60.0–60.5	0.816	OC	32.3	26.8	ET551[‡]	0.784 ± 0.028	1950 ± 290	1570–2300
			EC	22.8	18.9	ET555 [‡]	0.693 ± 0.051	2950 ± 590	2360–3850
122	60.5–61.2	0.758	OC	58.6	45.9	ET552 [‡]	$0.628 \pm 0.010^{\parallel}$	3740 ± 130	3910–4290
			EC	17.8	14.1	ET556 [‡]	0.641 ± 0.033	3570 ± 420	3380–4510
123	61.2–61.7	0.949	OC	52.9	50.6	ET554[‡]	0.657 ± 0.013	3370 ± 160	3460–3840
			EC	34.2	32.0	ET558 [‡]	0.690 ± 0.014	2980 ± 160	2960–3350
124	61.7–62.3	1.084	OC	18.2	20.1	ET692[‡]	0.401 ± 0.028	7340 ± 560	7610–8930
			EC	15.9	18.5	ET693 [‡]	0.413 ± 0.020	7110 ± 390	7600–8330
125	62.3–62.8	0.927	OC	65.9	61.5	ET694[‡]	$0.088 \pm 0.054^{\parallel}$	$>13\,100^{\parallel}$	$>15\,300^{\parallel}$
			EC	41.1	39.4	ET695 [‡]	0.237 ± 0.052	$11\,570 \pm 1760$	$11\,270\text{--}16\,260$

*Calculated subtracting procedural blank (see section 4.2); quantification error is $0.5\text{--}1.7\,\mu\text{g kg}^{-1}$.

[†]Calibrated using OxCal 4.1 (see section 3.2 and Figs 1 and 2).

[‡]TANDY AMS system (analysis of graphite processed from CO_2) (see section 3.2).

[§]Indistinguishable from modern values within a 1σ range.

[¶]Sample is probably contaminated. Yield after graphitization exceeds 100%.

^{||}Uncertainty and measured value are of similar size. Therefore, ages are shown as upper 2σ limits only (see section 4.3).

Note: Samples discussed in Jenk and others (2009) are marked in bold.

4. RESULTS AND DISCUSSION

4.1. OC and EC concentrations

OC and EC concentrations of the water-insoluble carbon fractions for Nevado Illimani and Colle Gnifetti ice cores are shown in Tables 1 and 2. For Colle Gnifetti, OC concentrations vary about a mean of $33\,\mu\text{g kg}^{-1}$ (range: $14\text{--}66\,\mu\text{g kg}^{-1}$), which is similar to previously reported values for Fiescherhorn (Jenk and others, 2006) and somewhat lower than the preindustrial background determined for Colle Gnifetti on a previous ice core (Lavanchy and others, 1999). EC concentrations are in general lower than OC concentrations. With mean values of about $22\,\mu\text{g kg}^{-1}$, they cover a range of $14\text{--}66\,\mu\text{g kg}^{-1}$, resulting in a mean OC/EC ratio of 1.6.

For Illimani, an abrupt shift is observed in the concentration records. Down to about 2 m above bedrock, concentrations show high and abrupt fluctuations about a mean of $132\,\mu\text{g kg}^{-1}$ (range: $80\text{--}242\,\mu\text{g kg}^{-1}$), which is substantially higher than the Colle Gnifetti average. However, the four lowermost samples show low concentrations of about $25\,\mu\text{g kg}^{-1}$. This points to massive changes in source strengths, related to large-scale changes within the climate system (see also section 4.5). EC concentrations are about

$36\,\mu\text{g kg}^{-1}$ for the upper part and $10\,\mu\text{g kg}^{-1}$ close to the bedrock. This results in a mean OC/EC ratio of 3.1, which is significantly higher than ratios obtained from the European mid-latitudes. The Amazon basin, as the largest single emitter of biogenic gases and particles from plants, is responsible for the increased burden of the aerosols with OC (Guyon and others, 2003).

For the Greenland ice-core samples, six of eight measured concentrations are in the range $0.9\text{--}5.1\,\mu\text{g kg}^{-1}$ after procedural blank subtraction (see section 4.2 for details). Quantification uncertainties for these concentrations are $0.8\text{--}1.0\,\mu\text{g kg}^{-1}$. Two samples show significantly higher concentrations of 19 and $42\,\mu\text{g kg}^{-1}$. While the latter was visibly contaminated by small particles, no such contamination was detected for the former. EC was not determined for the GRIP samples, as concentrations are thought to be $<0.2\text{--}2.0\,\mu\text{g kg}^{-1}$ (Chýlek and others, 1995; Hagler and others, 2007).

4.2. Procedural blank estimation

Procedural blanks accounting for contamination during sample processing were reproducible and resulted in a

Table 2. Summary of the Illimani 1999 ice-core samples, which were analysed by ^{14}C dating. Absolute uncertainties indicate the 1σ range

Core section	Depth m w.e.	Ice kg	Carbon fraction	Carbon $\mu\text{g kg}^{-1*}$	Carbon μg	AMS label	Radiocarbon f_M	^{14}C age years BP	Calibrated age [†] years BP = 1950
168	89.3–89.9	0.916	OC	89.0	83.1	EG0535	0.881 ± 0.009	1020 ± 80	800–1050
			EC	20.9	19.5	EG0565	0.863 ± 0.014	1180 ± 130	970–1260
169	89.9–90.5	0.631	OC	110.4	71.2	EG0539	0.873 ± 0.009	1090 ± 80	930–1120
			EC	22.5	14.5	EG0566	0.820 ± 0.016	1600 ± 160	1340–1690
180	97.0–97.3	0.390	OC	80.4	32.9	EG0452	0.852 ± 0.012	1290 ± 110	1080–1300
			EC	18.2	7.4	EG0567	0.895 ± 0.028	890 ± 250	570–1060
199	108.2–108.9	1.207	OC	83.9	102.8	EG0240	0.619 ± 0.006	3850 ± 80	4160–4410
			EC	Not analysed					
200	109.1–109.5	0.321	OC	232.9	76.3	EG0237	0.447 ± 0.007	6470 ± 120	7270–7480
			EC	Not analysed					
201	109.6–109.9	0.365	OC	241.5	89.7	EG0238	0.383 ± 0.006	7700 ± 120	8380–8600
			EC	Not analysed					
202	110.6–110.8	0.377	OC	122.7	47.8	EG0239	0.371 ± 0.009	7960 ± 190	8560–9070
			EC	81.7	31.1	EG0241	0.356 ± 0.008	8300 ± 190	9030–9480
203	111.2–111.4	0.450	OC	93.2	43.5	EG0320	0.310 ± 0.019	9410 ± 490	9920–11 400
			EC	38.6	17.7	EG0568	0.319 ± 0.010	9180 ± 260	9930–10 740
204	111.9–112.1	0.357	OC	24.2	10.2	EG0321	0.326 ± 0.037	9000 ± 910	9010–11 600
			EC	10.0	3.9	EG0574	0.333 ± 0.038	8840 ± 910	8780–11 240
205	112.3–112.5	0.411	OC	30.3	14.0	EG0322	0.393 ± 0.026	7510 ± 530	7840–9000
			EC	Not analysed					
205b	112.5–112.8	0.354	OC	16.8	7.5	EG0460	0.354 ± 0.046	8340 ± 1050	8060–10 770
			EC	7.6	3.0	EG0471	0.324 ± 0.051	9060 ± 1280	8770–12 140
206	112.9–113.1	0.344	OC	28.4	11.3	Sample lost during processing			
			EC	11.9	4.4	EG0575	0.259 ± 0.035	$10 870 \pm 1080$	11 180–14 090

*Calculated subtracting procedural blank (see section 4.2); quantification error is $0.5\text{--}1.7 \mu\text{g kg}^{-1}$.

[†]Calibrated using OxCal 4.1 (see section 3.2 and Figs 1 and 2).

mean carbon mass of $1.5 \pm 0.8 \mu\text{g OC}$ ($n=20$, standard deviation of the samples) per filter. This result matches the previously reported blank value of $1.3 \pm 0.6 \mu\text{g OC}$ (Jenk and others, 2007). Carbon masses of the blanks are independent of the masses of the artificial ice used. A procedural blank value of similar magnitude ($1.3 \mu\text{g}$ for TC, not including filter and graphitization blank) is reported by Drogg and others (2007), using a similar filtration technique to extract carbonaceous particles from glacier ice for radiocarbon determination. Although carbon masses show a slightly asymmetric distribution, we take the arithmetic mean and standard deviation for corrections. Uncertainties obtained with an asymmetric blank correction do not differ substantially. The f_M for the OC blank was 0.64 ± 0.11 ($n=9$). Recent aerosol samples from Zürich, Switzerland, give f_M values of ~ 0.6 (Szidat and others, 2004a). The contamination may therefore originate from the atmosphere, though the pathway into the sample is as yet unclear.

For EC, the procedural blank is $0.3 \pm 0.1 \mu\text{g}$ ($n=6$) per filter. An f_M of the blank of 0.3 ± 0.3 obtained by Jenk and others (2007) is used in this study.

f_M is independent of the mass of carbon, thus allowing use of the arithmetic mean for correction. The relative contribution of the blank correction to the final dating uncertainty is strongly dependent on the size of the samples. While for the smallest GRIP sample ($2.7 \mu\text{g}$) 60% of the total age uncertainty is due to the procedural blank correction, the relative contribution for the largest Illimani sample ($103.8 \mu\text{g}$) is only 4%.

4.3. Ages derived from ^{14}C analysis of OC

Ages derived after radiocarbon calibration show in general a continuous increase with depth (Figs 1 and 2; Tables 1 and 2). Deviations from this trend exist between 50 and 53 m w.e. at Colle Gnifetti and between 110 and 115 m w.e. at Illimani. This is not unexpected. Outliers typically occur with a probability of 5–10%, when measuring small samples of well-characterized organic material (Scott, 2003; Blaauw and Christen, 2005). When measuring carbonaceous particles at a microgram level, an even higher fraction of outliers must be expected. Outliers are likely explained by additional contamination. For Colle Gnifetti ice core, 2 of 12 samples were regarded as outliers. Sample CG107 gave a result indistinguishable from modern values. The large uncertainty is, on the one hand, due to the low carbon content ($7.3 \mu\text{g}$) of the sample and, on the other hand, to a period of recurring ^{14}C ages in the calibration curve during the last 500 years (Reimer and others, 2004). CG115/16 was dated 2000 years older than the two surrounding samples, and the slightly enhanced OC/EC ratio of 1.9 points to an additional contamination within the OC fraction. Also not shown in Figure 1 is the lowermost sample (CG125) of the Colle Gnifetti ice core. As described by Jenk and others (2009), a low yield was observed for the graphitization process, leading to high overall dating uncertainties. Thus only a conservative upper age limit of $>15.3 \text{ ka BP}$ based on the $^{14}\text{C}/^{12}\text{C}$ ratio plus 2σ could be defined for this sample, as suggested by Stuiver and Polach (1977). For the Illimani ice core, 1 of 11 samples (IL205) was regarded as an outlier,

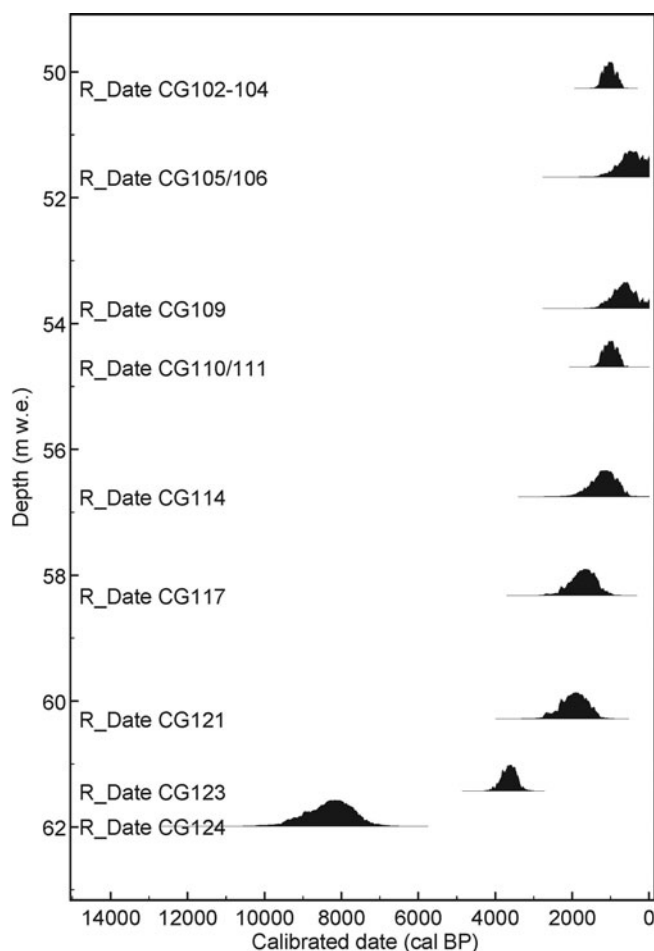


Fig. 1. Depth–age model for Colle Gnifetti ice-core ^{14}C data using OxCal 4.1 (Bronk Ramsey, 2001). The black distributions are probability density functions using the IntCal4.0 calibration curve (Reimer and others, 2004). The ages are calibrated years BP. The lowermost sample with a minimum age of >15 300 years cal BP (Table 1) is not shown here.

because of its too young radiocarbon age compared with the surrounding samples.

For both ice cores the ages cover a time-span from 1000 to >10 000 years. A strongly non-linear depth–age relationship is prominent in the lowermost part of the ice core, in agreement with the expected strong annual-layer thinning gradients towards bedrock typical for ice cores (Thompson and others, 1998). Samples close to bedrock are of Late Pleistocene age. Additional independent dating constraints corroborate that finding and assure the accuracy of the method (see section 4.5).

4.4. Ages derived from ^{14}C analysis of EC: is it necessary to separate the fractions?

The need to separate both fractions of particulate total OC prior to the radiocarbon determination was deduced from a previous study on Fiescherhorn ice core, consistently with EC fraction ages that are too old, even in time periods not affected by anthropogenic input of fossil carbon to the atmosphere (Jenk and others, 2006). Processes leading to the observed differences were poorly understood at that time. We therefore continued to determine $^{14}\text{C}/^{12}\text{C}$ ratios of EC for most of the ice-core samples analysed for OC. Results are shown in Figures 3 and 4. They corroborate that there are

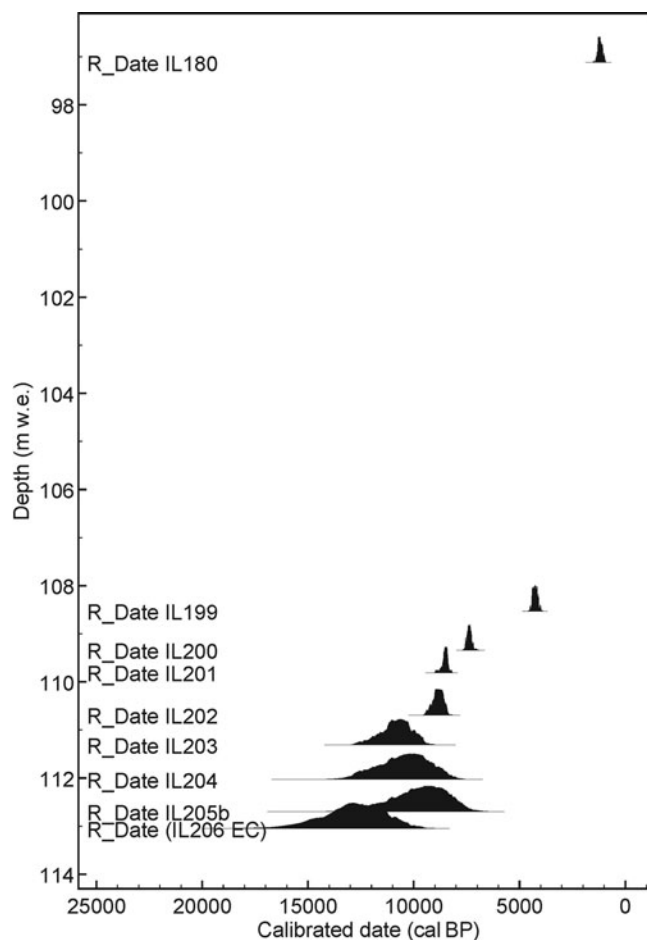


Fig. 2. Depth–age model for Nevado Illimani ice-core ^{14}C data using OxCal 4.1 (Bronk Ramsey, 2001). The series is based on the IntCal04 calibration curve (Reimer and others, 2004). Results for IL168 and IL169 are shown in Figure 5.

indeed samples with EC-derived ages older than the corresponding OC age. Some of the most pronounced age offsets of >1000 years resulted from the earliest measurements of Colle Gnifetti samples (e.g. CG114, CG117, CG121) on solid graphite targets using the same method set-up that has been used for the Fiescherhorn ice-core data. After excluding the ‘outliers’ mentioned above (CG107/109, CG115/116 and CG125) from the analysis, the total mean offset in the f_M values ($\Delta f_M = f_{MOC} - f_{MEC}$) is 0.007 ± 0.031 for Illimani and 0.030 ± 0.056 for Colle Gnifetti. Note that the means of the errors for the OC and EC fractions are ~ 0.025 . To evaluate whether the observed offset is significant and related to either the drilling site (Illimani/Colle Gnifetti) or the applied method (MICADAS/TANDY), we used two-tailed Student’s t and chi-square (χ^2) tests. Mean Δf_M values of Illimani are not found to be different from mean Δf_M values of Colle Gnifetti ($p=0.35$, two-sample assuming unequal variances). Accordingly, no significant differences in the mean between samples measured with the MICADAS or TANDY system can be observed ($p=0.25$). To test the hypothesis that there is no difference between f_M of OC and f_M of EC we use χ^2 test statistics. The null hypothesis being tested is that Δf_M is different from zero. Reduced chi-square values $\chi^2_{red} (\chi^2/df)$ are 2.15 ($N=7$; $p=0.01$ – 0.05) for Colle Gnifetti, 1.89 ($N=7$; $p=0.05$ – 0.20) for Illimani, 1.47 ($N=9$; r samples determined with the MICADAS system and

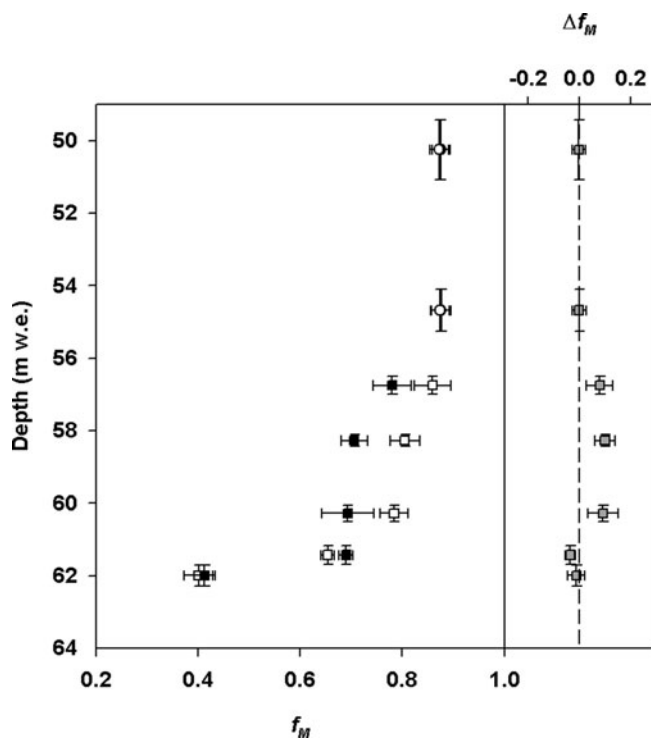


Fig. 3. f_M OC (white) and f_M EC (black) determined in seven sample pairs for Colle Gnifetti (circle: MICADAS CO_2 samples; squares: TANDY graphite samples), together with 1σ uncertainty ranges; grey squares mark the difference Δf_M (f_M OC– f_M EC), with the dotted line indicating a perfect match. Error bars on the depth axis describe the depth ranges for the single ice segments.

3.01 ($N=5$; $p=0.01$ – 0.05) for the TANDY system. Therefore, the difference between the observed results (Δf_M) and expected results ($\Delta f_M=0$) is not statistically significant on a 95% significance level for the Illimani and the MICADAS samples. Conversely, we conclude that for Colle Gnifetti and the TANDY samples the results could have been obtained by chance $<5\%$ of the time, and we reject the hypothesis that chance alone is responsible for the results.

We therefore ascribe the observed variations to two factors:

1. A systematic component may exist with small offset values arising from differences between the isotopic signature of OC and EC in atmospheric aerosols. While OC is thought to be emitted directly, the EC fraction is formed by pyrolysis and therefore exhibits the $^{14}\text{C}/^{12}\text{C}$ ratio inherent to the biomass at the time of combustion. Depending on the actual sources of EC, this ‘age reservoir’ can account for age offsets of decades to centuries (Gavin, 2001).
2. Dominating the variability is a random component that is controlled by either measuring artefacts produced by incomplete carbonate destruction, or additional contamination of OC or EC with either modern or fossil carbon. Direction and magnitude of those offsets are highly variable and not predictable.

Concerning the overall dating precision, it is desirable to use TC instead of the separated OC fraction, because of the higher carbon mass. If OC and EC resulted in the same ages, this would be justified. For Illimani, dating the ice core using

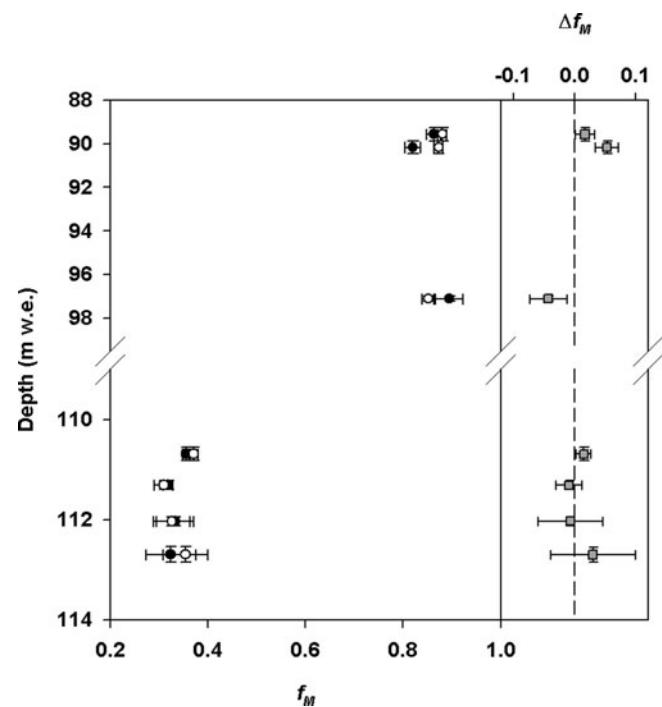


Fig. 4. f_M OC (white) and f_M EC (black) determined in seven sample pairs for Illimani, together with 1σ uncertainty ranges; grey squares mark the difference Δf_M (f_M OC– f_M EC). Error bars on the depth axis describe the depth ranges for the single ice segments.

EC (or TC) will result in similar depth–age models. However, due to some deviations for Colle Gnifetti not being sufficiently understood, we rely here solely on the ages derived from OC and we point out the need to always measure series of samples to correctly identify outliers as well as offsets.

4.5. Validation

Two possibilities exist to validate this new method: (1) an independently dated ice core can be dated accurately by applying our method; or (2) the measured ice cores offer independent dating options, in the best case overlapping with the ^{14}C -determined ice segments and matching their ages. Both approaches were followed, although several limitations obviously exist. Well-dated ice cores are rare and predominantly exist in polar regions, which are generally characterized by low atmospheric OC concentrations (Hagler and others, 2007). The ^{14}C results for the GRIP samples (Vinther and others, 2006) are shown in Table 3. In most cases, concentrations of OC are too low to yield meaningful dating results. Overall, results tend to be biased towards the procedural blank value ($f_M=0.64 \pm 0.11$). Old samples are dated too young; in contrast, young samples give ages that are too old. This indicates that the correction used may not be appropriate for these types of sample (large ice volumes, longer processing times). Therefore, although the results do not allow validation, the GRIP samples may serve to estimate the upper limit of the procedural blank, as they combine low carbon concentrations with physical properties of real ice samples.

As attempts to date the Greenland ice-core samples have so far failed, we base the validation of the new method on the following three lines of evidence.

Table 3. Summary of the Mercedario and GRIP ice-core samples, which were analysed by ^{14}C dating. Absolute uncertainties indicate the 1σ range

Core section	ALC age*	Ice	AMS label	Carbon OC	Radiocarbon	^{14}C date	$^{14}\text{C}_{\text{cal}}$ age [†]
	years BP	kg		μg	f_M	years BP	years BP
Mercedario (Andes, 6100 m a.s.l.; 31.97° S, 70.12° W)							
151	95 ± 10	0.755	EG0451	22.4	0.955 ± 0.019 [‡]	370 ± 160 [‡]	<550
152	100 ± 10	0.781	EG0459	9.0	0.913 ± 0.046	740 ± 400	320–1120
GRIP (Greenland, 3230 m a.s.l.; 72.58° N, 37.64° W)							
240–41	440 ± 1	1.277	EG0508	3.2	0.631 ± 0.212	3700 ± 2700	960–8420
439–40	950 ± 1	1.047	EG0817	3.3	0.778 ± 0.159	2020 ± 1640	540–4230
803–04	1932 ± 1	0.789	EG0815	5.6	0.336 ± 0.073	8770 ± 1750	8060–12 670
1143–44	2950 ± 3	1.124	EG0816	4.1	0.511 ± 0.108	5390 ± 1690	4090–8350
1447–48	3955 ± 6	1.119	EG0568	48.1	0.558 ± 0.008	4690 ± 120	5310–5580
2379–80	7933 ± 42	1.074	EG0546	21.9	0.472 ± 0.013	6030 ± 230	6640–7170
2526–27	8738 ± 58	1.361	EG0608	3.7	0.617 ± 0.090	3890 ± 1170	2960–5890
2626–27	9323 ± 70	1.288	EG0609	2.7	0.780 ± 0.271 [‡]	2000 ± 2790 [‡]	<6790

*Age based on annual layer counting.

[†]Calibrated using OxCal 4.1 (see section 4.5).[‡]Indistinguishable from modern values within a 1σ range.

4.5.1. Agreement between dating by annual-layer counting and radiocarbon

OC-derived ages calculated for the Fiescherhorn ice core (Jenk and others, 2006) before ~AD 1800 range from modern values to 1000 years, thus reasonably matching the depth-age model based on annual-layer counting. In the last 200 years the values are biased by the anthropogenic input of fossil carbon in the atmosphere. For Colle Gnifetti, dating based on annual-layer counting was only achievable for the last 200 years so that no overlap with unbiased radiocarbon-derived dating points was possible. The first two radiocarbon measurements of an ice core from Mercedario (31.97° S, 70.12° W; 6100 m a.s.l.) show ages well in line with a tentative chronology, based on annual-layer counting (Table 3). In contrast to the Alps, no anthropogenic bias is expected for the ~100-year old samples, since the ice-core site is remote from pollution sources.

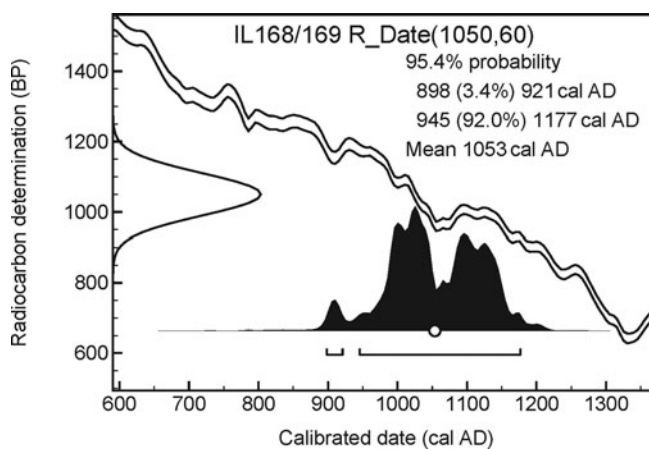


Fig. 5. Radiocarbon date of the combined Illimani samples IL168/169 (mean depth: 89.87 m w.e.) that include the volcanic signal of the unknown AD 1258 eruption (depth: 90.26 m w.e.) using OxCal 4.1 (Bronk Ramsey, 2001), based on the SHCal04 calibration curve (McCormac and others, 2004). The 2σ range spans AD 900–1180.

4.5.2. Agreement between dating by a volcanic horizon (AD 1258) and radiocarbon

In the Illimani ice core an exceptionally strong volcanic signature was detected at 90.26 m w.e. characterized by high concentrations of fluoride, sulfate and thallium (Kellerhals, 2008) and attributed to the major volcanic eruption in AD 1258 visible in various ice-core records (Clausen and others, 1997). Additional age control is given by an age based on annual-layer counting of AD 1250 ± 50 at this depth using the ECM record and by additional volcanic time markers throughout the ice-core archive (AD 1815, 1883, 1453). Two samples bracketing the AD 1258 time marker were analysed for their $^{14}\text{C}/^{12}\text{C}$ ratios (IL168 and IL169 in Table 2). The samples were measured very precisely, due to their large carbon contents of >70 μg each. Other than for the sample sequence shown in Figure 2, the Southern Hemispheric calibration curve (McCormac and others, 2004) was used for calibration. As both results were equal within their errors, they were combined in a weighted average and compared with the reference horizon. With a calibrated age of AD 1050 ± 70, the real age of AD 1258 is overestimated by only 200 ± 70 years (Fig. 5), which is an acceptable dating accuracy on the Holocene timescale. Possible explanations for the offset are summarized below.

4.5.3. Matching the Pleistocene/Holocene transition to independent ice-core chronologies

The last line of evidence arises from the presence of Last Glacial Stage ice in the Illimani ice core (Fig. 6). This is indicated by stronger depleted values in the record of stable isotopes (e.g. $\delta^{18}\text{O}$), which are coherent in several Andean ice-core archives (e.g. Huascarán, Peru (6048 m a.s.l.), and Sajama, Bolivia (6542 m a.s.l.)), and which were attributed to large-scale temperature changes during the end of the Pleistocene (Thompson and others, 1995, 1998). For Sajama, the timescale for the glacial portions of these archives was developed by matching records of $\delta^{18}\text{O}$ of the ice as well as $\delta^{18}\text{O}$ of the palaeo-atmospheric O_2 ($\delta^{18}\text{O}_{\text{atm}}$) with the respective Greenland Ice Sheet Project 2 (GISP2)

records (Sowers and Bender, 1995; Meese and others, 1997). Additional dating constraints arise from reproducible $^{14}\text{C}_{\text{AMS}}$ dates of wood embedded in the ice core (Thompson and others, 1998). Huascarán was dated by comparison with a ^{14}C -dated deep-sea foraminifera record of $\delta^{18}\text{O}_{\text{CaCO}_3}$ (Bard and others, 1987; Thompson and others, 1995). Strong similarity between the $\delta^{18}\text{O}$ record of Illimani and the other Andean stable-isotope records allows a comparison of the radiocarbon-derived timescale of Illimani to both independent timescales of Huascarán and Sajama, assuming temporal synchronicity. To achieve a continuous timescale out of discrete radiocarbon measurements, linear interpolation between the midpoints of the calibrated ^{14}C ranges was applied. Because the vial containing the lowermost OC sample (IL206) broke during measurement, for this depth we used the corresponding EC sample instead. Samples IL203, 204 and 205b, the dates of which are identical within their errors, were combined in a weighted average.

All records show a marked increase of $\delta^{18}\text{O}$, ending at ~ 10.5 ka BP, indicating the transition from a Pleistocene to a Holocene climate regime. This is in line with major-ion concentration data from Illimani (not shown) and the observed strong abrupt increase of carbonaceous aerosol concentrations (see section 4.1; Table 2), which both indicate major changes in the climate system. Starting in a wetter and cooler Last Glacial Stage, conditions along the eastern Andes became warm and dry during the Early Holocene (Baker and others, 2001; Abbott and others, 2003). Due to the low concentrations of $<10\ \mu\text{g}$ carbon for the two lowermost samples, only a tentative age of ~ 13 ka for the oldest ice on Illimani is suggested. However, due to the large uncertainty, we do not postulate a difference from previous dating attempts, which inferred an age of ~ 18 ka for the basal ice by wiggle-matching the Illimani δD record to the Huascarán $\delta^{18}\text{O}$ record.

To summarize, there is strong evidence that the evaluated method is suitable for ^{14}C measurements of OC in ice-core samples and that the ^{14}C ages are indeed representative for the age of the ice segments. Precision and accuracy are strongly controlled by the amount of available carbon. A small age offset towards too old ages may exist, indicated by the high-precision ^{14}C measurements that include a well-dated volcanic reference horizon. This can be due to an already altered isotopic signature of the aerosol at the time of deposition, either explained by 'inbuilt carbon ages' (Gavin, 2001) or by reservoir effects between primary emission and final deposition. Indications for the presence of 'old carbon' in atmospheric aerosols were found in an ocean sediment core drilled close to the northern African coast (Eglinton and others, 2002). OC that made up 1% of the mass of a known dust event was radiocarbon-dated with an age offset of ~ 1000 years compared with the sediment. This bias was attributed to the mobilization of altered OC compounds previously stored in the pedosphere and biosphere of the dust source regions. At Colle Gnifetti ice-core site, dry and wet deposition of Saharan dust frequently occurs in the present, and did throughout the past (Haeberli, 1977; Schwikowski and others, 1995; Wagenbach and others, 1996). Therefore an input of isotopically altered carbon together with the dust cannot be ruled out in principle. Taking Ca^{2+} and Al concentrations as proxies of the dust content, we estimate that 5–20% of the OC used for dating was transported together with the dust. Thus, age offsets of decades to centuries can be explained for Colle

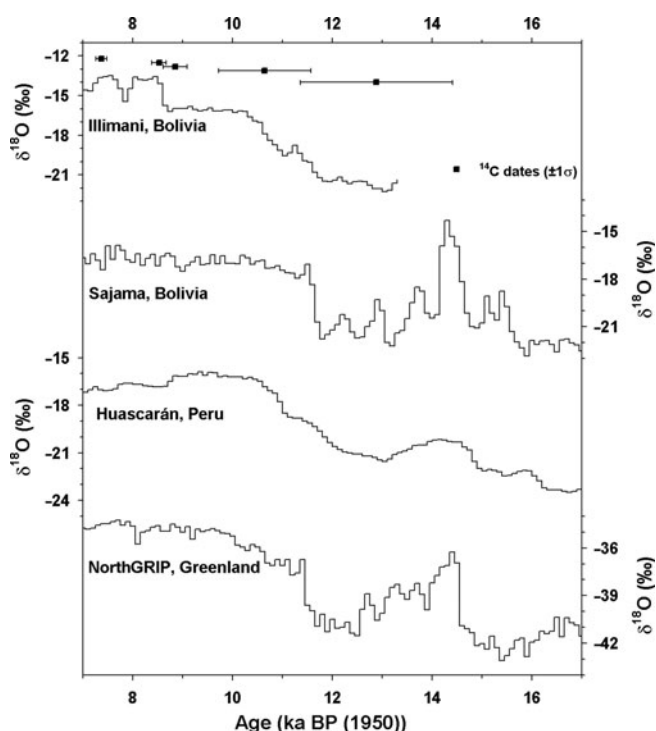


Fig. 6. 100 year averages of $\delta^{18}\text{O}$ from Illimani based on ^{14}C dates compared with 100 year averages of two tropical sites (Sajama and Huascarán) and one Northern Hemispheric site (NorthGRIP) with independent chronologies (Thompson and others, 1995, 1998; NorthGrip Members, 2004). All records show a strong increase in $\delta^{18}\text{O}$ at the Pleistocene–Holocene transition related to increasing temperatures. Assuming temporal synchronicity of the event among the archives, the ^{14}C -based Illimani timescale is reasonably accurate.

Gnifetti OC ages. Input of altered carbon may also be valid to explain the age deviation of ~ 200 years observed for the AD 1258 reference horizon of Illimani.

5. CONCLUSIONS

A recently developed new method to date ice cores using radiocarbon has proven to be a reliable tool for non-polar ice cores. This tool is strongly needed for developing timescales for ice cores, as appropriate dating options are scarce in many such palaeo-archives. Technical developments in AMS technologies nowadays allow measurement of sample sizes down to $3\ \mu\text{g}$, and form the basis for accurate and precise dating of small to ultra-small samples, which is the typical size range of carbon present in ice cores. OC concentrations in ice cores vary by several orders of magnitude, depending on the distance of the site from main carbon sources. For samples with low carbon content, precision and accuracy are strongly controlled by the required blank correction, giving the method low suitability for dating polar ice-core samples. Therefore, attempts to validate the method by dating GRIP ice-core samples with well-known ages failed. As the procedural blank is reproducible and can be estimated quantitatively together with its uncertainty, samples with at least $10\ \mu\text{g}$ of carbon can be dated properly. Thus, the method is suitable for various ice cores from the mid- and low latitudes close to major natural carbon sources. Ages obtained from $^{14}\text{C}/^{12}\text{C}$ ratios of both the OC fraction and the EC fraction show a

continuous increase with depth. The fraction of samples in disagreement with this trend is as expected, given the small sample sizes and the corresponding natural occurrence of outliers. When using this new method, it is necessary to analyse continuous sample sequences in order to identify outliers and offsets correctly. However, this is one of the major advantages of the method, since aerosols are constantly incorporated in the ice and samples can be extracted everywhere in the core. For Colle Gnifetti, the ^{14}C content of EC was in general slightly lower than for OC. This is in line with the expected longer residence time of EC in many media and the nature of pyrolytic formation of the EC aerosols, in contrast to dominantly biogenic emissions of OC. This finding justifies our separation of OC and EC fractions instead of using TC. For Illimani no significant differences between the two fractions was observed, allowing also the use of TC for age determination.

Accuracy of the method is assured through cross-validation within the Illimani ice-core archive, which offers independent dating constraints to check against the radiocarbon-derived ages. At the two considered time windows (AD 1258 and ~ 10.5 ka BP) a reasonable agreement exists between the two independent timescales.

The method is operational and offers a variety of possible future applications. In principle it may be valuable for any ice body that accumulated enough contemporary carbonaceous particles in the past and that remained undisturbed since then. Temporally, future applications are restricted to time periods prior to the beginning of major atmospheric release of fossil carbon to the atmosphere during industrialization. The method is valuable in particular for Holocene ice, where dating options that take advantage of the presence of glacial ice, using wiggle-matching approaches, fail.

Future investigations will be necessary to understand finally differences in the ^{14}C signature of OC and EC. Further efforts towards smaller reproducible blanks for the overall sample preparation procedure will remain a main issue, since at present they are still several orders of magnitude higher than the AMS measurement background. Additional improvements in the accuracy of the dating might be achievable in future by constraining radiocarbon ages with independent physically based glaciological models. The underlying concept is based on Bayesian statistics (Bronk Ramsey, 2008), and an increasing number of dating applications is actually arising that take advantage of merging radiometric and stratigraphic age information. Currently, an application to ice cores is mainly hampered by the lack of appropriate glacier-flow models for high-alpine environments.

ACKNOWLEDGMENTS

This work was supported by the National Centre of Competence in Research (NCCR) climate programme of the Swiss National Science Foundation (projects VITA and VIVALDI), the European Union Framework Programme 6 (FP6) project MILLENNIUM (017008) and the Istituto Nazionale per la Ricerca Scientifica e Tecnologica sulla Montagna (INRM). We thank the members of the drilling campaigns, P. Ginot, U. Schotterer, F. Stampfli, D. Stampfli, B. Zweifel, B. Francou, R. Gallaire, B. Pouyaud, P. Gabrielli, F. Planchon, B. Rufibach and A. Schwerzmann, for retrieving the ice cores. We thank the GRIP committee for providing ice for validation purposes.

REFERENCES

- Abbott, M.B. and 9 others. 2003. Holocene paleohydrology and glacial history of the central Andes using multiproxy lake sediment studies. *Palaeogeogr., Palaeoclimatol., Palaeoecol.*, **194**(1–3), 123–138.
- Alean, J., W. Haeberli and B. Schädler. 1983. Snow accumulation, firn temperature and solar radiation in the area of the Colle Gnifetti core drilling site (Monte Rosa, Swiss Alps): distribution patterns and interrelationships. *Z. Gletscherkd. Glazialgeol.*, **19**(2), 131–147.
- Baker, P.A. and 8 others. 2001. The history of South American tropical precipitation for the past 25,000 years. *Science*, **291**(5504), 640–643.
- Barbante, C. and 14 others. 2004. Historical record of European emissions of heavy metals to the atmosphere since the 1650s from alpine snow/ice cores drilled near Monte Rosa. *Environ. Sci. Technol.*, **38**(15), 4085–4090.
- Bard, E. and M. Frank. 2006. Climate change and solar variability: what's new under the sun? *Earth Planet. Sci. Lett.*, **248**(1–2), 1–14.
- Bard, E., M. Arnold, P. Maurice, J. Duprat, J. Moyes and J.C. Duplessy. 1987. Retreat velocity of the North Atlantic polar front during the last deglaciation determined by ^{14}C accelerator mass spectrometry. *Nature*, **328**(6133), 791–794.
- Biegalski, S.R., L.A. Currie, R.A. Fletcher, G.A. Klouda and R. Weissenböck. 1998. AMS and microprobe analysis of combusted particles in ice and snow. *Radiocarbon*, **40**(1), 3–10.
- Blaauw, M. and J.A. Christen. 2005. The problems of radiocarbon dating. *Science*, **308**(5728), 1551–1553.
- Bronk Ramsey, C. 2001. Development of the radiocarbon program. *Radiocarbon*, **43**(2A), 355–363.
- Bronk Ramsey, C. 2008. Deposition models for chronological records. *Quat. Sci. Rev.*, **27**(1–2), 42–60.
- Brook, E.J. 2005. Tiny bubbles tell all. *Science*, **310**(5752), 1285–1287.
- Chýlek, P., B. Johnson, P. Damiano, K.C. Taylor and P. Clement. 1995. Biomass burning record and black carbon in the GISP2 ice core. *Geophys. Res. Lett.*, **22**(2), 89–92.
- Clausen, H.B. and 6 others. 1997. A comparison of the volcanic records over the past 4000 years from the Greenland Ice Core Project and Dye 3 Greenland ice cores. *J. Geophys. Res.*, **102**(C12), 26,707–26,723.
- Currie, L.A. 2000. Evolution and multidisciplinary frontiers of ^{14}C aerosol science. *Radiocarbon*, **42**(1), 115–126.
- De Angelis, M., J. Simões, H. Bonnaveira, J.D. Taupin and R.J. Delmas. 2003. Volcanic eruptions recorded in the Illimani ice core (Bolivia): 1918–1998 and Tambora periods. *Atmos. Chem. Phys. Discuss.*, **3**(3), 2,427–2,463.
- Donahue, D.J., T.W. Linick and A.J.T. Jull. 1990. Isotope-ratio and background corrections for accelerator mass spectrometry radiocarbon measurements. *Radiocarbon*, **32**(2), 135–142.
- Döschner, A., H.W. Gäggeler, U. Schotterer and M. Schwikowski. 1996. A historical record of ammonium concentrations from a glacier in the Alps. *Geophys. Res. Lett.*, **23**(20), 2741–2744.
- Drosg, R., W. Kutschera, K. Scholz, P. Steier, D. Wagenbach and E.M. Wild. 2007. Treatment of small samples of particulate organic carbon (POC) for radiocarbon dating of ice. *Nucl. Instrum. Meth. Phys. Res. B*, **259**(1), 340–344.
- Eglinton, T.I., G. Eglinton, L. Dupont, E.R. Sholkovitz, D. Montluçon and C.M. Reddy. 2002. Composition, age, and provenance of organic matter in NW African dust over the Atlantic Ocean. *Geochem. Geophys. Geosyst.*, **3**(8), 3050. (10.1029/2001GC000269.)
- Eichler, A. and 7 others. 2000. Glaciochemical dating of an ice core from upper Grenzgletscher (4200 m a.s.l.). *J. Glaciol.*, **46**(154), 507–515.
- Eisen, O., U. Nixdorf, L. Keck and D. Wagenbach. 2003. Alpine ice cores and ground penetrating radar: combined investigations for glaciological and climatic interpretations of a cold Alpine ice body. *Tellus B*, **55**(5), 1007–1017.

- EPICA Community Members. 2004. Eight glacial cycles from an Antarctic ice core. *Nature*, **429**(6992), 623–628.
- Fagerli, H., M. Legrand, S. Preunkert, V. Vestreng, D. Simpson and M. Cerqueira. 2007. Modeling historical long-term trends of sulfate, ammonium, and elemental carbon over Europe: a comparison with ice core records in the Alps. *J. Geophys. Res.*, **112**(D23), D23S13. (10.1029/2006JD008044.)
- Gäggeler, H., H.R. von Gunten, E. Rössler, H. Oeschger and U. Schotterer. 1983. ^{210}Pb -dating of cold Alpine firn/ice cores from Colle Gnifetti, Switzerland. *J. Glaciol.*, **29**(101), 165–177.
- Gavin, D.G. 2001. Estimation of inbuilt age in radiocarbon ages of soil charcoal for fire history studies. *Radiocarbon*, **43**(1), 27–44.
- Graham, B. and 15 others. 2003. Composition and diurnal variability of the natural Amazonian aerosol. *J. Geophys. Res.*, **108**(D24), 2765. (10.1029/2003JD004049.)
- Guyon, P. and 6 others. 2003. In-canopy gradients, composition, sources, and optical properties of aerosol over the Amazon forest. *J. Geophys. Res.*, **108**(D18), 4591. (10.1029/2003JD003465.)
- Guyon, P. and 6 others. 2004. Sources of optically active aerosol particles over the Amazon forest. *Atmos. Environ.*, **38**(7), 1039–1051.
- Haeblerli, W. 1977. Sahara dust in the Alps – a short review. *Z. Gletscherkd. Glazialgeol.*, **13**(1–2), 206–208.
- Haeblerli, W. and J. Alean. 1985. Temperature and accumulation of high altitude firn in the Alps. *Ann. Glaciol.*, **6**, 161–163.
- Hagler, G.S.W., M.H. Bergin, E.A. Smith, J.E. Dibb, C. Anderson and E.J. Steig. 2007. Particulate and water-soluble carbon measured in recent snow at Summit, Greenland. *Geophys. Res. Lett.*, **34**(16), L16505. (10.1029/2007GL030110.)
- Jenk, T.M. and 7 others. 2006. Radiocarbon analysis in an Alpine ice core: record of anthropogenic and biogenic contributions to carbonaceous aerosols in the past (1650–1940). *Atmos. Chem. Phys.*, **6**(12), 5381–5390.
- Jenk, T.M. and 6 others. 2007. Microgram level radiocarbon (^{14}C) determination on carbonaceous particles in ice. *Nucl. Instrum. Meth. Phys. Res. B*, **259**(1), 518–525.
- Jenk, T.M. and 9 others. 2009. A novel radiocarbon dating technique applied to an ice core from the Alps indicating late Pleistocene ages. *J. Geophys. Res.*, **114**(D14), D14305. (10.1029/2009JD011860.)
- Kellerhals, T. 2008. Holocene climate fluctuations in tropical South America deduced from an Illimani ice core. (PhD thesis, University of Bern.)
- Knüsel, S. and 8 others. 2003. Dating of two nearby ice cores from the Illimani, Bolivia. *J. Geophys. Res.*, **108**(D6), 4181. (10.1029/2001JD002028.)
- Knüsel, S., S. Brütsch, K.A. Henderson, A.S. Palmer and M. Schwikowski. 2005. ENSO signals of the twentieth century in an ice core from Nevado Illimani, Bolivia. *J. Geophys. Res.*, **110**(D1), D01102. (10.1029/2004JD005420.)
- Lavanchy, V.M.H., H.W. Gäggeler, U. Schotterer, M. Schwikowski and U. Baltensperger. 1999. Historical record of carbonaceous particle concentrations from a European high-alpine glacier (Colle Gnifetti, Switzerland). *J. Geophys. Res.*, **104**(D17), 21,227–21,236.
- Legrand, M. and others. 2007. Major 20th century changes of carbonaceous aerosol components (EC, WinOC, DOC, HULIS, carboxylic acids, and cellulose) derived from Alpine ice cores. *J. Geophys. Res.*, **112**(D23), D23S11. (10.1029/2006JD008080.)
- Lugauer, M. and 6 others. 1998. Aerosol transport to the high Alpine sites Jungfraujoch (3454 m a.s.l.) and Colle Gnifetti (4452 m a.s.l.). *Tellus B*, **50**(1), 76–92.
- Lüthi, M.P. and M. Funk. 2001. Modelling heat flow in a cold, high-altitude glacier: interpretation of measurements from Colle Gnifetti, Swiss Alps. *J. Glaciol.*, **47**(157), 314–324.
- Masson-Delmotte, V. and 8 others. 2009. GRIP deuterium excess reveals rapid and orbital-scale changes in Greenland moisture origin. *Science*, **309**(5731), 118–121.
- Maupetit, F., D. Wagenbach, P. Weddeking and R.J. Delmas. 1995. Seasonal fluxes of major ions to a high altitude cold alpine glacier. *Atmos. Environ.*, **29**(1), 1–9.
- McConnell, J.R. and 9 others. 2007. 20th-century industrial black carbon emissions altered Arctic climate forcing. *Science*, **317**(5843), 1381–1384.
- McCormac, F.G., A.G. Hogg, P.G. Blackwell, C.E. Buck, T.F.G. Higham and P.J. Reimer. 2004. SHCal04 southern hemisphere calibration, 0–11.0 cal kyr BP. *Radiocarbon*, **46**(3), 1087–1092.
- Meese, D.A. and 8 others. 1997. The Greenland Ice Sheet Project 2 depth–age scale: methods and results. *J. Geophys. Res.*, **102**(C12), 26,411–26,423.
- Muscheler, R., F. Joos, J. Beer, S.A. Müller, M. Vonmoos and I. Snowball. 2007. Solar activity during the last 1000 yr inferred from radionuclide records. *Quat. Sci. Rev.*, **26**(1–2), 82–97.
- North Greenland Ice Core Project (NorthGRIP) Members. 2004. High-resolution record of Northern Hemisphere climate extending into the last interglacial period. *Nature*, **431**(7005), 147–151.
- Oeschger, H., U. Schotterer, B. Stauffer, W. Haeblerli and H. Röthlisberger. 1977. First results from Alpine core drilling projects. *Z. Gletscherkd. Glazialgeol.*, **13**(1–2), 193–208.
- Parrenin, F. and 26 others. 2007. The EDC3 chronology for the EPICA Dome C ice core. *Climate Past*, **3**(3), 485–497.
- Ramirez, E. and 12 others. 2003. A new Andean deep ice core from Nevado Illimani (6350m), Bolivia. *Earth Planet. Sci. Lett.*, **212**(3–4), 337–350.
- Reddy, C.M. and 8 others. 2002. Radiocarbon as a tool to apportion the sources of polycyclic aromatic hydrocarbons and black carbon in environmental samples. *Environ. Sci. Technol.*, **36**(8), 1774–1782.
- Reimer, P.J. and 28 others. 2004. IntCal04 terrestrial radiocarbon age calibration, 0–26 cal kyr BP. *Radiocarbon*, **46**(3), 1029–1058.
- Ruff, M., L. Wacker, H.W. Gäggeler, M. Suter, H.-A. Synal and S. Szidat. 2007. A gas ion source for radiocarbon measurements at 200 kV. *Radiocarbon*, **49**(2), 307–314.
- Ruff, M., S. Szidat, H.W. Gäggeler, M. Suter, H.-A. Synal and L. Wacker. In press. Gaseous radiocarbon measurements of small samples. *Nucl. Instrum. Meth. Phys. Res. B*. (10.1016/j.nimb.2009.10.032.)
- Santos, G.M., R.B. Moore, J.R. Southon, S. Griffin, E. Hinger and D. Zhang. 2007a. AMS C-14 sample preparation at the KCCAMS/UCI facility: status report and performance of small samples. *Radiocarbon*, **49**(2), 255–269.
- Santos, G.M., J.R. Southon, S. Griffin, S.R. Beaupre and E.R.M. Druffel. 2007b. Ultra small-mass AMS C-14 sample preparation and analyses at KCCAMS/UCI Facility. *Nucl. Instrum. Meth. Phys. Res. B*, **259**(1), 293–302.
- Schwikowski, M., P. Seibert, U. Baltensperger and H.W. Gäggeler. 1995. Study of an outstanding Saharan dust event at the high-Alpine site Jungfraujoch, Switzerland. *Atmos. Environ.*, **29**(15), 1829–1842.
- Schwikowski, M., A. Döschner, H. Gäggeler and U. Schotterer. 1999. Anthropogenic versus natural sources of atmospheric sulphate from an Alpine ice core. *Tellus B*, **51**(5), 938–951.
- Scott, E.M. 2003. The Third International Radiocarbon Intercomparison (TIRI) and the Fourth International Radiocarbon Intercomparison (FIRI) – 1999–2002 results, analysis and conclusions. *Radiocarbon*, **45**(2), 135–328.
- Seinfeld, J.H. and S.N. Pandis. 1998. *Atmospheric chemistry and physics: from air pollution to climate change*. New York, John Wiley and Sons.
- Slater, J.F., L.A. Currie, J.E. Dibb and B.A. Benner, Jr. 2002. Distinguishing the relative contribution of fossil fuel and biomass combustion aerosols deposited at Summit, Greenland through isotopic and molecular characterization of insoluble carbon. *Atmos. Environ.*, **36**(28), 4463–4477.

- Sodemann, H., A.S. Palmer, C. Schwierz, M. Schwikowski and H. Wernli. 2006. The transport history of two Saharan dust events archived in an Alpine ice core. *Atmos. Chem. Phys.*, **6**(3), 667–688.
- Sowers, T. and M. Bender. 1995. Climate records covering the last deglaciation. *Science*, **269**(5221), 210–214.
- Steier, P. and 6 others. 2006. Radiocarbon determination of particulate organic carbon in non-temperated, alpine glacier ice. *Radiocarbon*, **48**(1), 69–82.
- Stuiver, M. and H.A. Polach. 1977. Discussion: reporting of C-14 data. *Radiocarbon*, **19**(3), 355–363.
- Synal, H.-A., S. Jacob and M. Suter. 2000. The PSI/ETH small radiocarbon dating system. *Nucl. Instrum. Meth. Phys. Res. B*, **172**(1–4), 1–7.
- Synal, H.-A., M. Stocker and M. Suter. 2007. MICADAS: A new compact radiocarbon AMS system. *Nucl. Instrum. Meth. Phys. Res. B*, **259**(1), 7–13.
- Szidat, S. and 10 others. 2004a. Radiocarbon (^{14}C)-deduced biogenic and anthropogenic contributions to organic carbon (OC) of urban aerosols from Zürich, Switzerland. *Atmos. Environ.*, **38**(24), 4035–4044.
- Szidat, S. and 11 others. 2004b. Source apportionment of aerosols by ^{14}C measurements in different carbonaceous particle fractions. *Radiocarbon*, **46**(1), 475–484.
- Szidat, S. and 6 others. 2004c. THEODORE, a two-step heating system for the EC/OC determination of radiocarbon (^{14}C) in the environment. *Nucl. Instrum. Meth. Phys. Res. B*, **223–224**, 829–836.
- Szidat, S. and 7 others. 2006. Contributions of fossil fuel, biomass-burning, and biogenic emissions to carbonaceous aerosols in Zurich as traced by ^{14}C . *J. Geophys. Res.*, **111**(D7), D07206. (10.1029/2005JD006590.)
- Thompson, L.G. and 7 others. 1995. Late glacial stage and Holocene tropical ice core records from Huascarán, Peru. *Science*, **269**(5220), 46–50.
- Thompson, L.G. and 11 others. 1998. A 25,000-year tropical climate history from Bolivian ice cores. *Science*, **282**(5395), 1858–1864.
- Thompson, L.G. and 10 others. 2002. Kilimanjaro ice core records: evidence for Holocene climate change in Tropical Africa. *Science*, **298**(5593), 589–593.
- Thompson, L.G. and 8 others. 2006a. Abrupt tropical climate change: past and present. *Proc. Natl. Acad. Sci. USA (PNAS)*, **103**(28), 10,536–10,543.
- Thompson, L.G. and 6 others. 2006b. Ice core evidence for asynchronous glaciation on the Tibetan Plateau. *Quat. Int.*, **154–155**, 3–10.
- Vinther, B.M. and 12 others. 2006. A synchronized dating of three Greenland ice cores throughout the Holocene. *J. Geophys. Res.*, **111**(D13), D13102. (10.1029/2005JD006921.)
- Wacker, L., M. Christl and H.-A. Synal. In press. Bats: a new powerful tool for AMS data reduction. *Nucl. Instrum. Meth. Phys. Res. B*. (10.1016/j.nimb.2009.10.078.)
- Wagenbach, D. and K. Geis. 1989. The mineral dust record in a high altitude Alpine glacier (Colle Gnifetti, Swiss Alps). In Leinen, M. and M. Sarnthein, eds. *Paleoclimatology and paleometeorology: modern and past patterns of global atmospheric transport*. Dordrecht, etc., Kluwer Academic Publishers, 543–564. (NATO ASI Series C: Mathematical and Physical Sciences 282.)
- Wagenbach, D., S. Preunkert, J. Schaefer, W. Jung and L. Tomadin. 1996. Northward transport of Saharan dust recorded in a deep Alpine ice core. In Guerzoni, S. and R. Chester, eds. *The impact of African dust across the Mediterranean*. Dordrecht, etc., Kluwer Academic Publishers, 291–300.
- Wagner, S. 1994. Three-dimensional flow and age distribution at a high-altitude ice-core drilling site. In Haeberli, W. and B. Stauffer, eds. *Proceedings of the ESF/EPC Workshop on Greenhouse Gases, Isotopes and Trace Elements in Glaciers as Climate Evidence for Holocene*, 27–28 October 1992, Zürich. Zürich, VAW Arbeitsheft.

MS received 12 March 2009 and accepted in revised form 20 October 2009